UNLIMITED

BR 114930

ROYAL AEROSPACE ESTABLISHMENT

Technical Report TR 90033

July 1990

Sustained-Load Crack Growth of 8090 Aluminium-Lithium Alloy Plate in Dry Air at 50-200°C

by

S. P. Lynch

UNLIMITED

90 10 31 025

ROYAL AEROSPACE ESTABLISHMENT

Technical Report 90033

Received for printing 10 July 1990

SUSTAINED-LOAD CRACK GROWTH OF 8090 ALUMINIUM-LITHIUM ALLOY PLATE IN DRY AIR AT 50-200°C

by

S. P. Lynch*

SUMMARY

The effects of test temperature, stress-intensity factor, sodium impurity content, and ageing condition on the short-transverse sustained-load (creep) cracking of pre-cracked Al-Li-Cu-Mg-Zr (8090) alloy plate have been studied. Creep cracking was orders of magnitude faster, and threshold stress-intensity factors were much lower, than for conventional aluminium alloys such as 2014-T651. Significant rates of cracking were observed in 8090 alloys at temperatures as low as 60°C at stress-intensity factors as low as ~5 MPa$\sqrt{m}$. For a given stress-intensity factor, cracking rates were similar for underaged, peak-aged, and overaged conditions, but were higher for alloys with higher sodium impurity levels. Metallographic and fractographic observations suggest that the presence of liquid, sodium-rich impurity phases promote creep cracking in 8090 alloys. Creep cracking in conventional Al-alloys is probably exacerbated by solid impurity phases such as lead, which are less mobile and therefore less damaging than sodium-rich phases. *Grant B. Ta· ·· , TT) ←*

Departmental Reference: Materials/Structures 288

---

* The present work was done while the author was attached to RAE from the Aeronautical Research Laboratory, Defence Science and Technology Organisation, Melbourne, Australia

LIST OF CONTENTS

1   INTRODUCTION

The development of Al-Li base alloys as lower density, higher stiffness replacements for conventional Al alloys has concentrated mainly on producing satisfactory performance at ~20°C. Most room-temperature properties of recent commercial Al-Li alloys appear to be at least as good as conventional Al alloys, with the exception of short-transverse fracture toughness which was addressed in Ref 1. There has been relatively little work on the performance of Al-Li alloys at elevated temperatures, despite potential applications such as for airframe components near engines in subsonic aircraft, for airframes for supersonic aircraft, and for some space hardware. The limited work which has been carried out at elevated temperatures includes studies of tensile properties at temperatures up to 300°C, and at 20°C after soaking at elevated temperatures[2,3]. Some studies of creep deformation[4] and creep crack growth[5-7] have also been carried out.

Strengthening precipitates in 8090 Al-Li-Cu-Mg-Zr alloys (δ' and S') coarsen relatively slowly compared with those in conventional 2xxx and 7xxx Al alloys and, hence, strength is maintained up to higher temperatures, and for longer hold times at elevated temperatures, for 8090 alloys. For example, strength is maintained up to 160°C for long term (1000h) soaking[3]. Precipitation of S' on sub-grain boundaries, which prevents dynamic recovery, and thermal restoration of order in the δ' precipitates also contribute to the maintenance of elevated temperature strength[3].

Studies of creep crack growth in Al-Li base alloys, on the other hand, suggest that the resistance to cracking is lower than in conventional alloys when there are relatively planar, continuous intergranular crack paths normal to the applied stress. For Al-Li-Cu-Mg-Zr extrusions, creep cracking at 150°C was faster than in conventional alloys for the T-L orientation but slower for the L-T orientation[5]. Crack bifurcation along the planar grain boundaries of the T-L plane was responsible for the resistance to cracking of the L-T orientation. Creep cracking in Al-Li plate along the short-transverse (S-L) plane has also been reported at temperatures as low as 20°C[7]. Cracking at 80°C in dry air was more extensive than at 20°C and was observed down to low stress-intensity factors (~6 MPa$\sqrt{m}$). Conventional Al alloys are not known to exhibit creep crack growth in dry air at 20°C except when embrittling metal impurity phases such as lead are present[8-10]. Sodium-rich phases are known to be present in Al-Li alloys[11,12], but the mechanisms of creep cracking and whether embrittling phases are involved, have not been established.

In the present work, creep crack growth in commercial and experimental Al-Li-Cu-Mg-Zr (8090) plates has been studied and compared with cracking in conventional Al alloys. Cracking along the short-transverse (S-L) plane was examined since it was expected that this orientation would be the most susceptible. The effects on creep cracking of sodium impurity content and ageing treatments (including double-ageing treatments which increase fracture toughness as described in Ref 1) were examined. The aim of the work was to establish the kinetics of cracking as a function of stress-intensity factor and temperature, and to determine the mechanisms of cracking.

2   EXPERIMENTAL PROCEDURE

2.1   Materials and heat-treatments

(a) Two commercial 8090 plates (Table 1), also used for the studies of short-transverse fracture toughness[1], were used in this work. Most tests were carried out on material aged 32h at 170°C, but other ageing treatments, including the double-ageing treatments described in Ref 1, were also used.

(b) Three experimental Al-Li alloy plates (36 mm thick), containing different trace amounts of sodium (Table 1), which had been cast and fabricated at RAE were also studied. The experimental alloys were solution-treated, quenched, naturally aged for several years and then artificially aged 32h at 170°C.

(c) Some creep tests were also carried out on 2014-T651 and 7010-T7351 (conventional) aluminium alloy plates for comparison with the 8090 alloys.

2.2   Testing and examination

Bolt-loaded double-cantilever-beam (DCB) specimens, as used for fracture-toughness testing, were also used for creep tests. Specimens were pre-cracked so that initial stress-intensity-factor (K_1) values were near the (critical) fracture toughness value. The specimens were then held at temperatures from 50-200°C in dry air (using a silica gel desiccant for temperatures <100°C) until sustained-load cracking stopped. Crack growth was monitored on the polished side surfaces of specimens by scribing the positions of the crack tip (to an accuracy ~0.1 mm) at intervals during crack growth. The positions of the scribe lines were then measured using a travelling microscope at the end of the test. Crack velocities at high K_1 were also calculated from the time to produce creep crack growth increments of several millimetres, which were measured on fracture

surfaces between increments of overload fracture*. Fracture surfaces were examined by optical microscopy, scanning-electron micr scopy (SEM), and secondary-ion mass spectroscopy (SIMS).

Stress-intensity factors were calculated from the equation given in Rcf 1. Loading displacements 'v' were routinely measured at 20°C since initial tests showed that differences in thermal expansion between the alloy and the steel bolts did not cause measurable changes to 'v' over the temperature range studied. Values of 'E' used were 70 GPa for the 2014 alloy, 80 GPa for 8090 at 20°C, 75 GPa for 8090 at 170°C, and values between 75 and 80 GPa for 8090 at intermediate temperatures[2].

3   RESULTS

3.1 Kinetics of cracking

For commercial and experimental 8090 alloy plates (aged 32h ac 170°C', crack velocities, $\dot{a}$, were constant for certain ranges of stress-intensity factor, K_1 . These 'plateau-velocities' were smaller at lower K_1 ranges, and a threshold K_1 value, below which cracking did not occur, was observed (Fig 1). There was a small amount of scatter in $\dot{a}$ for a given K_1 range, and in K_1 values at which $\dot{a}$ changed from one plateau value to another, for specimens tested under nominally the same conditions. Thus, scatter bands for data from three to four specimens shown in subsequent Figures do not show the plateaux at lower K_1 ranges. Crack velocities at a given K_1 increased with increasing temperature, but threshold values were 3-4 MPa$\sqrt{m}$ for the commercial alloys at all testing temperatures (Fig 2). Cracking rates were appreciable (~10 mm/yr) even at temperatures as low as 60°C and stress-intensity factors as low as 5 MPa$\sqrt{m}$.

Rates of cracking at a given temperature and K_1 value for 8090 material initially aged for different times (24-100h) at 170°C were not significantly different. However, double-aged material (32h at 170°C + 5 min at 200°C + CWQ) with double the toughness of single-aged material[1], behaved differently from single-aged material. For double-aged material, creep crack growth at the highest K_1 used for testing single-aged material (16 MPa$\sqrt{m}$) occurred only after an incubation period. These incubation periods (which were not observed for single-aged material) depended on the testing temperature, and corresponded

---

* At 200°C, where rates of cracking were high, specimens were rapidly heated, held for 5 min, and then quenched. Subsequent overload 'pop-in' required approximately twice the loading displacement to that required previously. This observation led to the work described in Ref 1.

to the times approaching those which caused complete re-embrittlement (see Ref 1). Initial rates of cracking were then slower, but after times which produced complete re-embrittlement, rates were similar to those observed for single-aged material for equivalent K_1 values.

For single-aged experimental alloys, rates of creep cracking at a given temperature and K_1 value were 3-5 times higher for the alloy with ~40 ppm sodium than for the alloys with ~10 ppm sodium (Fig 3). Furthermore, the fracture toughness of material with ~40 ppm sodium was only about half that for material with ~10 ppm sodium. The two alloys (G15 and G16) with ~10 ppm sodium behaved similarly.

For conventional aluminium alloys, data in the literature[13] and data obtained in the present work, showed that rates of S-L creep cracking at equivalent temperatures and K_1 values were orders of magnitude slower than those observed for 8090 alloys. Threshold K_1 values were also considerably higher for conventional alloys than for 8090 alloys (Fig 4).

Arrhenius plots of creep crack velocity for given values of K_1 versus 1/T gave activation energies of ~0.89 eV from 50-120°C, and ~0.58 eV from 120-200°C for both the commercial 8090 alloy plates (Fig 5). Activation energies for experimental alloys with high and low sodium contents were similar to each other and to the commercial alloys (Fig 6). An activation energy of 0.35 eV was calculated for creep cracking of the 2014 alloy at high K_1, which is the same as that found for creep cracking of an Al-Mg-Si alloy doped with lead impurities[10] (Fig 7). The significance of these values is discussed in section 4.3.

3.2 Metallographic and fractographic observat.ons

Creep crack growth in Al-Li alloy plates produced multiple, parallel intergranular cracks, particularly at high K_1 values (Fig 8). Fracture surfaces had a 'flaky' appearance (Fig 9) because some grains had been lifted above the general fracture plane due to tearing of uncracked ligaments behind the main crack front. Observations on the side surface of the experimental alloy with ~40 ppm sodium showed that brittle intergranular cracks occurred around inclusions at considerable distances ahead of the main crack tip. Deformation and fracture of ligaments between some of these cracks then occurred (Fig 10).

Fracture surfaces produced by creep crack growth at 50-200°C at high K_1 in commercial and experimental 8090 plates exhibited numerous, brittle intergranular islands, often centred on inclusions and surrounded by dimpled areas (Fig 11). Cracking at low K_1 also produced brittle islands but they were not

as obvious as those produced at high K_1 because dimples around the islands were smaller and shallower than those produced at high K_1 .

Brittle islands were only rarely observed after overload fracture of the commercial alloys but were observed after overload of the experimental alloys (Fig 12). However, they were smaller and less numerous than those observed after creep cracking (for the same test temperature). For overload fracture, there were more brittle islands for the alloy with the higher sodium content, and islands were not observed after testing at temperatures $\leq -78°C$ (Fig 13). SIMS observations of overload fracture surfaces, produced in situ under high vacuum, for the 25mm commercial plate showed that there were discrete sodium rich areas (Fig 14). The other materials were not examined by SIMS.

For the 2014-T651 plate, S-L creep crack growth at 80-170°C produced 'brittle' intergranular regions and dimpled areas, but discrete brittle islands were less well defined than those for 8090 alloys; overload fracture of 2014 plate produced well defined dimples on fracture surfaces (Fig 15).

4   DISCUSSION

Before discussing the mechanisms and kinetics of creep cracking, and the reasons for the inferior creep cracking resistance of 8090 alloys compared with conventional Al alloys, mechanisms of overload fracture are discussed. The observations for overload cracking, particularly in the experimental alloys with different sodium levels, help to establish the form of the impurities and their effects on fracture-surface appearance. The role of impurities during creep crack growth is then discussed.

4.1   Mechanisms of overload fracture

The fractographic observations for the commercial alloys indicated that fracture occurred by a localised microvoid-coalescence process for some boundaries (producing well-defined dimpled fracture surfaces), and by 'brittle' intergranular fracture for others. The effect of various microstructural features on overload crack growth in the commercial 8090 alloys was discussed in Ref 1. It was concluded that brittle intergranular fracture and low fracture toughness was caused primarily by lithium segregation at grain boundaries. The presence of grain-boundary precipitate-free zones (PFZ) and precipitates also played an important role in the fracture process by causing strain localisation and facilitating nucleation of voids, respectively.

For the experimental alloy with ~40 ppm sodium, liquid-metal embrittlement (LME) due to sodium-rich phases appears to be the major cause of low fracture

toughness, although the other features undoubtedly contribute. The toughness of this material was only ~8 MPa$\sqrt{m}$, whereas the toughness of the material with 5-10 ppm sodium, with otherwise similar composition and microstructure, was ~16 MPa$\sqrt{m}$. Aluminium alloys are known to be embrittled by liquid Na-K alloys since wetting the external surfaces of stressed specimens induces brittle intergranular and cleavage-like fractures in alloys which do not exhibit such features when they are tested in dry air[14]. Aluminium alloys with high levels of sodium are also known to contain liquid sodiu...-rich phases.

Liquid phases (rich in Na and K) at grain boundaries in Al-Li alloys con-taining ≥40 ppm Na have been identified by TEM and energy-dispersive x-ray analysis (EDXA) of thin foils[11,12]. The phases were lenticular (~1 μm long), appeared lighter than their surroundings, and sometimes contained mobile bubbles of gas indicating that the phases were liquid at 20°C. For commercial alloys with low sodium-impurity levels (≤5 ppm), lenticular phases (~0.08 μm long) which appeared lighter than their surroundings were also observed. These phases were too small to be analysed by EDXA, but were probably rich in alkali-metal impuri-ties since SIMS of intergranular fracture surfaces showed that discrete Na-K rich phases were present[12]. SIMS observations of fracture surfaces of the 25mm com-mercial plate studied in the present work also revealed the presence of sodium-rich areas (Fig 14).

The brittle intergranular islands centred on inclusions and surrounded by dimpled areas on fracture surfaces of the experimental alloys* are probably caused by LME due to the presence of Na-K rich phases adjacent to inclusions. This conclusion is consistent with observations that: (i) more islands were present for the alloy with the higher sodium level and (ii) fewer islands were present after overload at lower temperatures, with islands absent at testing temperatures ≤ -78°C . Furthermore, only **liquid** embrittling phases have the mobility to keep up with rapid overload fracture -- surface diffusion of embrit-tling atoms from solid phases would not be able to keep up with rapid (>10 mm/s) cracking. The progressive decrease in the number of brittle islands with decreasing temperature (down to -78°C) suggests that the embrittling phases had a range of compositions (melting-points), with some of them containing embrittling elements besides Na and K. (Pure sodium melts at 98°C, binary Na-K phases can be liquid down to -13°C, and Na-K-Cs phases can be liquid down to -78°C[11].)

---

* Transgranular cleavage-like islands have also been observed on fracture surfaces of Al-Li and other Al alloys containing sodium[14-16].

4.2 Mechanisms of creep cracking in Al alloys

The metallographic and fractographic observations for the commercial and experimental 8090 alloys suggest that creep crack growth involves relatively brittle cracking radiating from inclusions followed by more ductile cracking, so that brittle islands surrounded by dimples are observed on fracture surfaces. As discussed above for overload fracture, the islands are probably caused by LME due to the presence of sodium-rich phases. The brittle intergranular islands are larger and more numerous after creep crack growth than after overload (at the same test temperature), probably because cracks 'run out of' embrittling metal after a smaller extent of crack growth under overload conditions than under creep conditions.

Cracks probably run out of liquid metal when the centre of the liquid meniscus behind the crack tip comes into contact with the crack tip. The shape of the meniscus will depend on the crack velocity and, for a given volume of liquid in cracks, the meniscus may break down after smaller increments of crack growth during rapid overload fracture than for slow creep cracking (Fig 16). Overload cracks may also run out of liquid after smaller crack extensions because overload cracks are blunter than creep cracks. Under creep conditions, embrittling atoms could also migrate to crack tips by surface diffusion, and this could occur when the phases are liquid or solid. However, most Na-K rich phases are likely to be liquid during creep at 50-200°C.

For the commercial alloys studied in this work, with ≤5 ppm Na + K, liquid impurity phases are probably sufficiently small that their presence facilitates creep crack growth but not rapid overload fracture. For the RAE experimental alloys, sodium-rich phases are present in sufficient amounts to have a small effect on rapid fracture for alloys with ~10 ppm sodium and a large effect on rapid fracture for alloys with ~40 ppm sodium, as well as to facilitate creep cracking.

Alkali-metal and other impurities are present in Al-Li alloys (Table 1) because the aluminium and the lithium themselves initially contain these impurities. Impurities can also be picked up from fluxes and refractories during melting and casting. The levels of alkali-metal impurities in recently produced commercial Al-Li alloys, however, are similar to the levels often found in other aluminium alloys, although the form of the impurities appears to be different. In many aluminium alloys, there is sufficient silicon available to produce a high-melting-point Na-Al-Si compound. In Al-Mg alloys, where silicon preferentially forms a compound with magnesium (Mg_2Si), bismuth is added so that a

Na-Bi compound is formed[17]. For Al-Li alloys, the activity of elements which form compounds with sodium is probably low due to their preferential compound formation with lithium so that low-melting-point sodium-rich phases are present.

Creep crack growth in conventional Al alloys is probably also associated with the presence of embrittling impurities since fracture surfaces exhibited similar features to those observed for 8090 alloys, although brittle islands were less well defined. However, sodium-rich liquid phases are not likely to be present, as discussed above. Other impurity elements which could promote cracking in Al alloys include Pb, In, Sn and Cd[18,19]. In conventional alloys, solid Pb-rich impurity phases are sometimes present, and detailed studies of creep cracking in Al-Mg-Si alloys[9,10] have shown that such phases promote cracking. For the 2014 alloy studied in the present work, the identity and distribution of impurity phases have not been established, but analysis showed that the alloy contained ~12 ppm lead which could be sufficient to promote creep cracking. The activation energy for cracking in 2014 also suggests that lead is responsible, as discussed in the following section.

It has been argued in previous work[20-22] that embrittling atom facilitate crack growth by adsorbing at crack tips and weakening interatomic bonds, thereby facilitating dislocation injection from crack tips and promoting the coalescence of cracks with small voids ahead of cracks. This explanation is consistent with the presence of small dimples sometimes observed on 'brittle' fracture surfaces, and with the observations of substantial slip on planes intersecting cracks[20-22]. Alternative explanations for LME, eg based on adsorption facilitating tensile separations of atoms (atomically brittle decohesion)[19], are not consistent with such observations. Under creep conditions, adsorption-induced weakening of interatomic bonds probably facilitates the thermally activated injection of dislocations from cracks tips and thereby promotes the growth of voids.

Deformation and fracture of ligaments between impurity-induced cavities is also necessary for cracking and probably involves 'normal' thermally activated dislocation processes, and cavity formation in PFZ around grain-boundary precipitates. For 8090 alloys, creep fracture of ligaments, like overload fracture, is probably facilitated by lithium segregation at grain boundaries. Such an effect could explain why double-aged specimens exhibited incubation periods prior to creep cracking since it was proposed in Ref 1 that double-ageing decreased lithium segregation at grain boundaries and that re-segregation occurred during subsequent exposure at 60-170°C.

4.3 Kinetics of creep cracking and embrittlement in Al-Li and other Al alloys

Sub-critical crack growth of conventional (7075-T651) Al alloys due to the presence of an 'unlimited' external supply of liquid metal (mercury) occurs at very high velocities ($\sim 2 \times 10^{-1}$ m/s) for K_1 values in the range 5-20 MPa$\sqrt{m}$, and threshold K_1 values are only 1-2 MPa$\sqrt{m}$ [23] . For LME of other materials, lower plateau-velocities, à , and higher K_1 threshold values have been observed, eg à $\sim 5 \times 10^{-2}$ m/s for Ti alloys in mercury[24], à $\sim 10^{-4} - 10^{-5}$ m/s for D6ac steel in mercury[25]. The rate-controlling processes have not been established, although the rate of capillary flow to crack tips could limit the velocity for 7075 Al in mercury.

For sub-critical cracking of 7075-T651 Al alloy due to the presence of an external supply of solid metal (indium), and for solid-metal induced embrittlement of other materials, it has been shown that rates of cracking are controlled by surface self-diffusion of embrittling atoms to crack tips[18]. Effective values of the surface-diffusion coefficient are $\sim 10^{-14}$ m^2/s at homologous temperatures ~ 0.5 and are $\sim 10^{-10}$ m^2/s at temperatures just below the melting point[18]. Thus, average crack growth rates for short cracks (~ 10 μm) can be quite high ($\sim 10^{-5}$ m/s) at temperatures just below the melting point.

For creep crack growth in Al-Mg-Si alloys containing Pb-rich phases, an activation energy for creep cracking of 0.35 eV was reported[10], and this is consistent with cracking controlled by multilayer surface-diffusion of lead from lead-rich phases to crack tips[22]. An equation, $\dot{a} \approx r_p \cdot 2D_s/x^2$, where à is the creep crack velocity, r_p is the size of the plastic zone (in which creep cavities are nucleated), D_s is the surface-diffusion coefficient, and x is the diffusion distance from the lead-rich phase to the point at which coalescence with other cavities occurs (ie about half the spacing between the embrittling phases), also gives crack velocities in the range found experimentally[22]. For the 2014 alloy, the activation energy for cracking was about the same as that for cracking of Al-Mg-Si alloys containing lead, and is consistent with surface self-diffusion of lead to tips of cavities being the rate-controlling process, as for Al-Mg-Si alloys.

For Al-Li alloys, creep crack growth is probably not controlled by transport of embrittling atoms to crack tips since capillary flow (when phases are liquid) or surface diffusion of sodium (when phases are solid) would be fast enough to produce crack velocities many orders of magnitude greater than those observed. The decrease in the slope of the Arrhenius plots for creep cracking in 8090 alloys above 120°C suggests that cracking involves two other (slower)

consecutive kinetic processes, with the same rates at ~120°C but different activation energies. Further work is required to identify these processes, but localised creep deformation and fracture between impurity-induced cavities are probably involved. This would be consistent with the inhibiting effect on creep cracking of double-ageing which increases fracture toughness.

Overall rates of creep cracking in 8090 alloys would, on the above basis, be dependent on the rate of creep fracture of ligaments between impurity-induced cavities and on the area of the ligaments -- with the latter affecting the former since smaller ligaments would be subjected to higher stresses. The area of ligaments will depend on the volume and spacing of impurity phases and these areas will be smaller for material with the higher sodium content. The higher creep cracking rates for the experimental alloy with the higher sodium content can be explained along these lines. The higher creep cracking rates for 8090 alloys compared with conventional alloys presumably occur because the rate-controlling processes are faster for 8090 (Fig 17). Notwithstanding that creep deformation and fracture of ligaments is probably the rate-controlling step in 8090 alloys, the presence of liquid, sodium-rich phases are essentially responsible for the faster rates than those in conventional alloys since they result in rapid formation of cavities separated by highly stressed ligaments.

If the inferior S-L creep cracking resistance of Al-Li alloys compared with conventional alloys is primarily caused by the presence of Na-rich impurity phases as discussed above, then there is probably little that can be done to improve the creep cracking resistance. The level of sodium impurity in commercial alloys is generally less than 5 ppm, and achieving lower levels would probably not be economically viable. Furthermore, attempts to 'tie-up' the sodium impurity as a high-melting-point compound by adding other elements would probably fail due to preferential compound formation between the additions and lithium, as already mentioned.

The practical implications of the present work are hard to assess. The studies have involved exposure of pre-cracked material stressed normal to the short transverse grain orientation at elevated temperatures -- a situation that is rare in practical components. Furthermore, data from the literature[3] indicate that Al-Li alloys, such as 8090, exhibit better tensile properties at elevated temperatures than the Al-Cu alloys they are intended to replace. Conventional creep tests using smooth specimens also show that the resistance of Al-Li alloys to creep deformation is better than that in conventional Al alloys[26]. Thus, the poor short-transverse creep-cracking resistance of Al-Li alloy plate may not be a serious limitation for most anticipated uses.

5   CONCLUSIONS

(1)   Sub-critical (creep) cracking 8090 plate along the short-transverse plane is much faster, and threshold stress-intensity factors are much lower, than in conventional aluminium alloys. Significant rates of cracking can occur at temperatures as low as 60°C at stress-intensity factors as low as 5 MPa$\sqrt{m}$ for plate stressed normal to the short-transverse plane.

(2)   Creep-crack-growth rates in 8090 alloys are similar for underaged, peak-aged, and overaged conditions (for one-step ageing), but were initially much lower after double ageing. Creep-crack velocities are 3-5 times higher for alloys with ~40 ppm sodium than for alloys with ~10 ppm sodium, for a given stress-intensity factor.

(3)   Creep fracture surfaces of 8090 alloys are characterised by brittle inter-granular islands which are centred on inclusions and surrounded by dimpled regions.

(4)   The presence of liquid sodium-rich impurity phases adjacent to inclusions promotes creep crack growth in 8090 alloys. The phases are too small to affect overload fracture in commercial 8090 alloys but can facilitate both overload and creep cracking in alloys with ~40 ppm sodium.

(5)   Creep cracking in 2014 conventional Al alloys is probably promoted by solid impurity phases such as lead which are less mobile and damaging than liquid phases.

(6)   Impurity atoms facilitate crack growth probably because they migrate to crack tips, weaken interatomic bonds, and thereby facilitate dislocation injection from crack tips.

(7)   The rate-controlling processes for cracking were probably localised creep and fracture between impurity induced cavities for 8090 alloys, and probably surface-diffusion of impurities to tips of cavities for conventional alloys.

Acknowledgments

14

Table 1

COMPOSITIONS OF MATERIALS USED. TRACE IMPURITIES WERE DETERMINED BY ATOMIC ABSORPTION SPECTROSCOPY; (< INDICATES ELEMENT WAS BELOW THE LIMIT OF DETECTABILITY.)

	wt%						ppm by wt						
	Li	Cu	Mg	Zr	Fe	Si	Na	K	Pb	In	Sn	Cd	Ca
8090 25mm plate	2.39	1.26	0.73	0.10	0.04	0.03	5	<1	<10	20	<20	3	<10
8090 45mm plate	2.54	1.17	0.68	0.12	0.04	0.06	3	2	<10	20	50		
RAE alloy G17	2.48	1.13	0.69	0.13	0.01	0.01	40-44	<1.	<10	20	<20	3	<10
RAE alloy G16	2.53	1.14	0.70	0.12	0.01	0.01	10						<10
RAE alloy G15	2.42	1.09	0.72	0.1	0.03	0.03	5-10	<1	<10	30	<20	4	<10

REFERENCES

No.	Author	Title, etc
1	S. P. Lynch	Fracture of 8090 Aluminium-Lithium alloy plate: Short-transverse fracture toughness. RAE TR90035 and Mater. Sci. and Engng., to be published. (1990)
2	B. Noble S. J. Harris K. Harlow	Mechanical properties of Al-Li-Mg alloys at elevated temperatures. Aluminium-Lithium alloys II, edited by T. H. Sanders Jr and E. A. Starke Jr, pp 65-77 (1984)
3	M. Pridham B. Noble S. J. Harris	Elevated temperature strength of Al-Li-Cu-Mg alloys. Aluminium-Lithium alloys III, edited by C. Baker, P. J. Gregson, S. J. Harris and C. J. Peel, pp 547-554 (1986)
4	K. T. Park E. J. Lavernia F. A. Mohamed	Creep behaviour of an aluminium-lithium alloy. Aluminium-Lithium alloys V, edited by E. A. Starke Jr and T. H. Sanders Jr, pp 1155-1160 (1989)
5	K. Sadananda K. V. Jata	Creep crack growth behaviour of two Al-Li alloys. *Metall. Trans. A.* **19A**, pp 847-854 (1988)
6	K. V. Jata	Creep crack growth resistance of 2091 Al-Li alloy. Aluminium-Lithium alloys V, edited by E. A. Starke Jr and T. H. Sanders Jr *Materials and Components Engng. Publ.,* Warely, England (1989)
7	N. Bengood H. Cai J. T. Evans N. J. H. Holroyd	Microcrack nucleation and sustained-loading crack growth in Al-Li alloys. *Mater. Sci. and Engng.* **A119**, pp 23-32 (1989)
8	M. Guttmann B. Quantin Ph. Dumoulin	Intergranular creep embrittlement by non-soluble impurity: Pb in precipitation hardened Al-Mg-Si alloys. *Metal. Sci.* **17**, pp 123-140 (1983)

References (continued)

No.	Author	Title, etc
9	J. J. Lewandowski V. Kohler N. J. H. Holroyd	Effects of lead on the sustained-load cracking of Al-Mg-Si alloys at ambient temperatures. *Mater. Sci. and Engng.* **96**, pp 185-195 (1987)
10	J. J. Lewandowski Y. S. Kim N. J. H. Holroyd	Pb-induced solid metal embrittlement of Al-Mg-Si alloys at temperatures of -4°C to 80°C. *Metall. Trans. A,* to be published
11	D. Webster	The effect of low melting point impurities on the properties of aluminium-lithium alloys. *Metall. Trans. A.* **18A**, pp 2181-2193 (1987)
12	D. Webster	Temperature dependence of toughness in various aluminium-lithium alloys. Aluminium-Lithium alloys III, edited by C. Baker, P. J. Gregson, S. J. Harris and C. J. Peel (1986)
13	J. L. Kenyon G. A. Webster J. C. Radon C. E. Turner	An investigation of the application of fracture mechanics to creep cracking. In: Creep and Fatigue in Elevated Temperature Applications. *Inst. of Mech Engrs. Conf. Publ. 13,* (1974)
14	D. N. Fager M. V. Hyatt H. T. Diep	A preliminary report on cleavage in Al-Li alloys. *Scripta Metall.* **20**, pp 1159-1164 (1986)
15	S. P. Lynch	Unpublished work (1989)
16	W. S. Miller M. P. Thomas J. White	Sodium induced cleavage fracture in high strength aluminium alloys. *Scripta. Metall.* **21**, pp 663-668 (1987)
17	D. E. J. Talbot C. E. Ransley	The addition of bismuth to aluminium-magnesium alloys to prevent embrittlement by sodium. *Metall. Trans. A,* **8A**, pp 1149-1154 (1977)
18	S. P. Lynch	Solid-metal-induced embrittlement of aluminium alloys and other materials. *Mater. Sci. and Engng.* **A108**, pp 203-212 (1989)
19		Embcittlement by liquid and solid metals, edited by M. H. Kamdar. *Met. Soc. AIME,* Warrendale, Pa. (1984)

References   (concluded)

No.	Author	Title, etc
20	S. P. Lynch	Mechanisms of stress corrosion cracking and liquid metal embrittlement in Al-An-Mg bicrystals. *J. Mater. Sci.*, **20**, pp 3329-3338 (1985)
21	S. P. Lynch	Environmentally assisted cracking: overview of evidence for an adsorption-induced localised-slip process. *Acta Metall.* **36**, pp 2639-2661 (1988)
22	S. P. Lynch	Mechanisms of intergranular fracture. *Mater. Sci. Forum*, **46**, pp 1-24 (1989)
23	M. O. Speidel	Current understanding of stress corrosion crack growth in aluminium alloys. In: The theory of stress corrosion cracking in alloys, edited by J. C. Scully, NATO Brussels, pp 289-344 (1971)
24	J. A. Feeney M. J. Blackburn	The status of stress corrosion cracking of titanium alloys in aqueous solutions. *Ibid*, pp 355-398
25	S. P. Lynch	Metallographic and fractographic aspects of liquid-metal embrittlement. In: Environmental degradation of engineering materials in aggressive environments, eds. M. R. Louthan Jr., R. P. McNitt and R. D. Sission Jr. *Virginia Polytechnic Inst.*, pp 229-244 (1981)
26	C. J. Peel	Private Communication

Fig 1
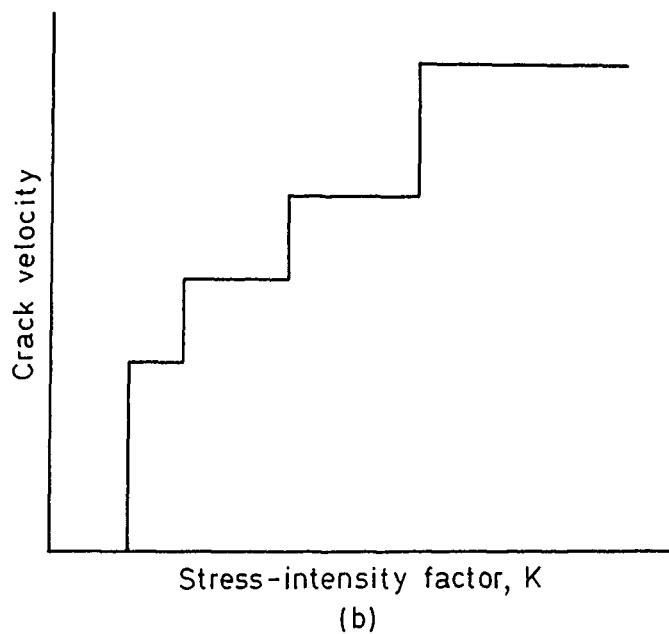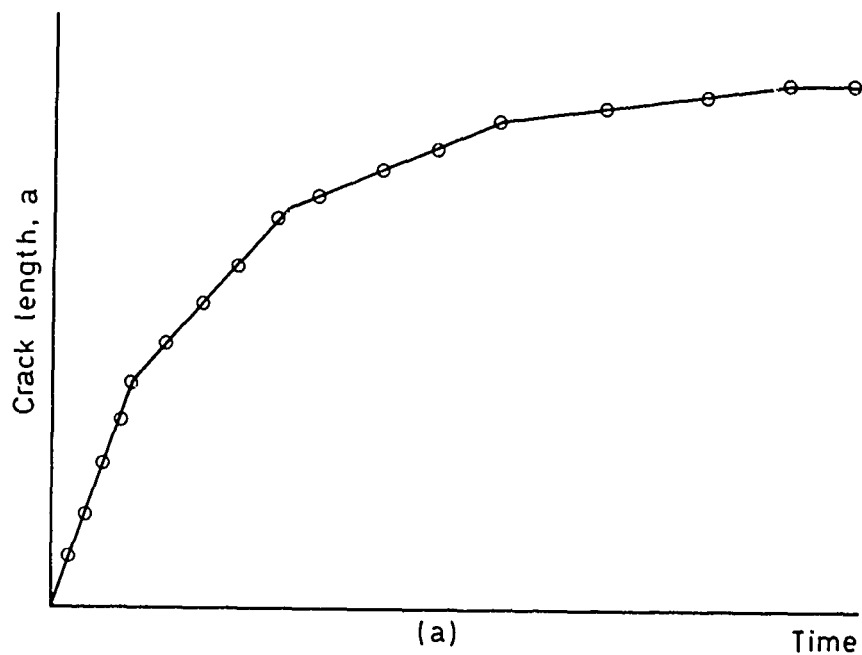
Fig 1 (a) crack length versus time, and (b) corresponding crack velocity versus stress-intensity factor plots typically obtained for S-L creep crack growth in bolt-loaded DCB specimens
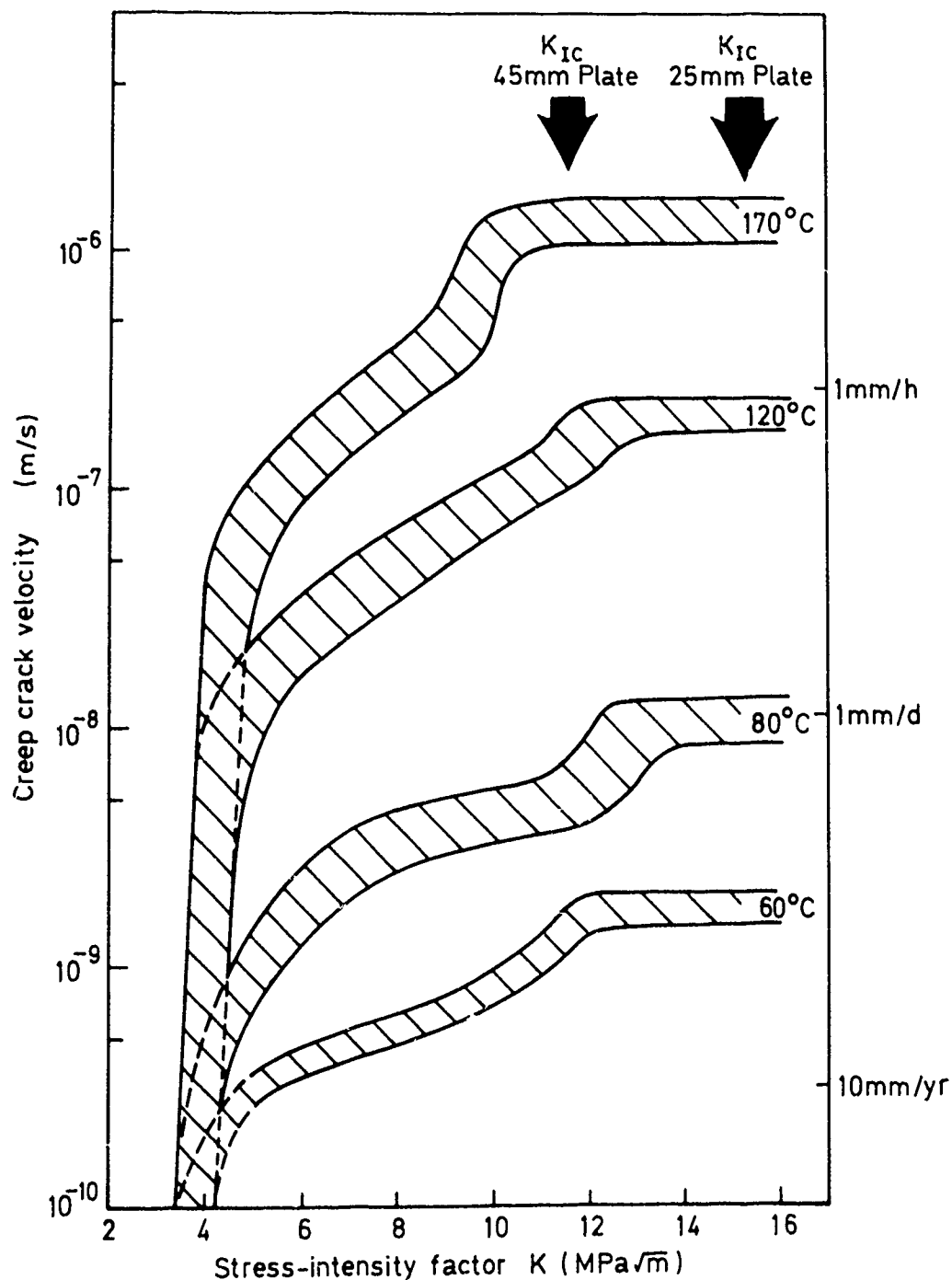
Fig 2

Fig 2 Creep-crack-velocity versus stress-intensity-factor data for 8090 specimens (aged 32h at 170°C) from 25 and 45mm plates cracked along the short-transverse plane at 60-170°C
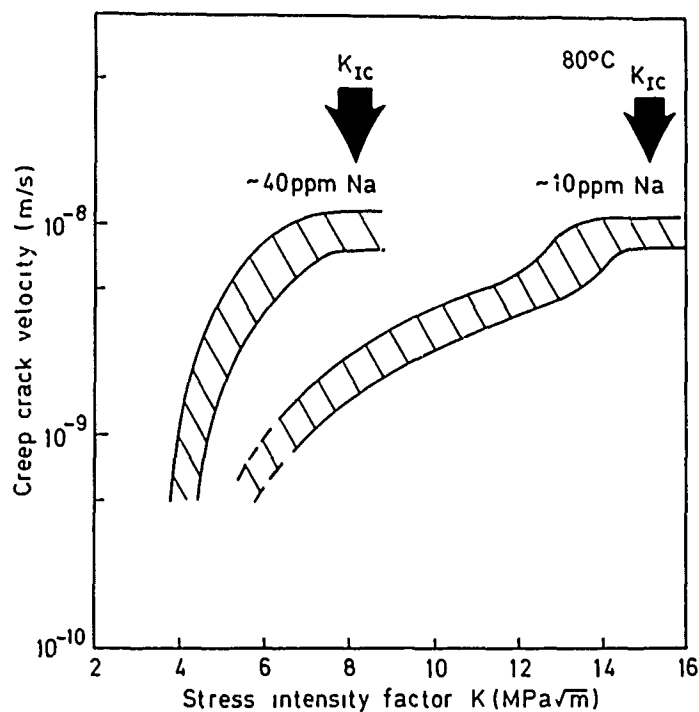
Fig 3 S-L creep-crack-velocity at 80°C versus stress-intensity-factor data for experimental alloys (aged 32h at 170°C) with ~40 ppm sodium impurity
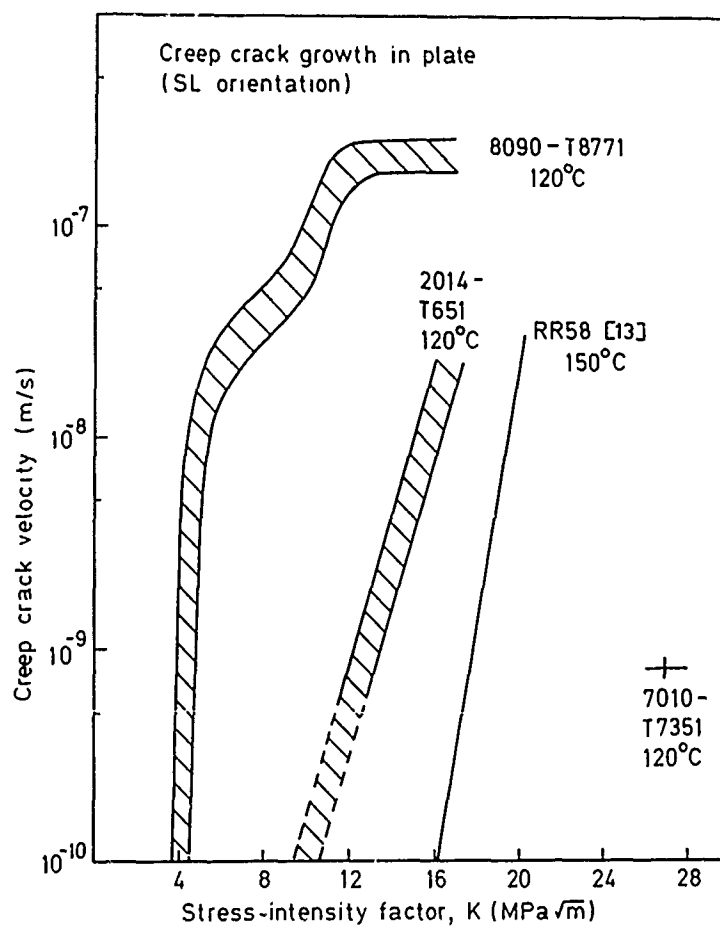
Fig 4 S-L creep-crack-velocity versus stress-intensity-factor data for several conventional commercial aluminium alloys compared with the 8090 Al-Li alloy

TR 90033
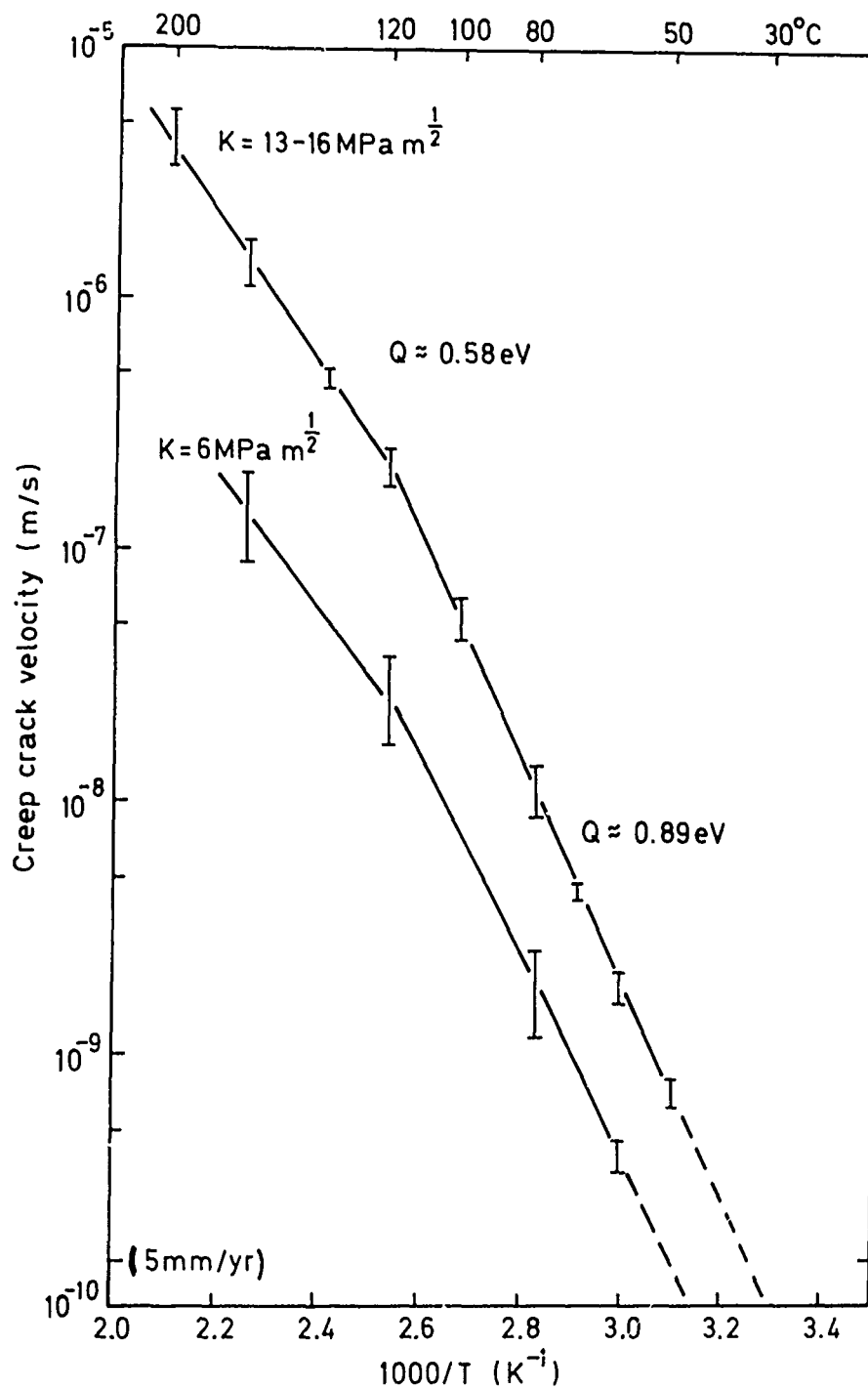
Fig 5

Fig 5 Arrhenius plots of S-L creep-crack-velocity at K values of 6 and 13-16 MPa√m versus inverse absolute temperature for 8090 commercial alloy plates
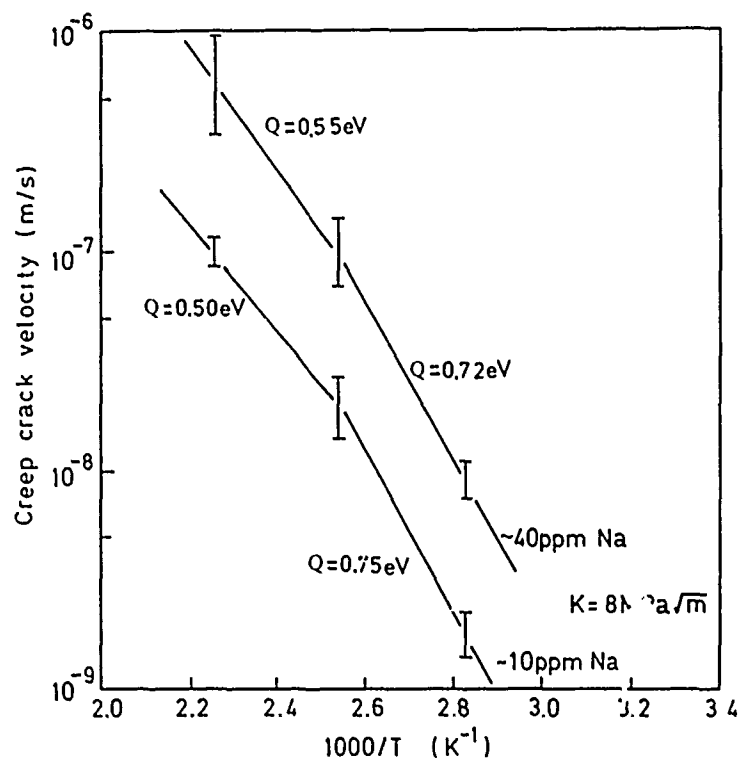
Fig 6 Arrhenius plots of S-L creep-crack-velocity at a K value of 8 MPa√m versus inverse absolute temperature for experimental 8090 alloys with ~10 and ~40 ppm sodium
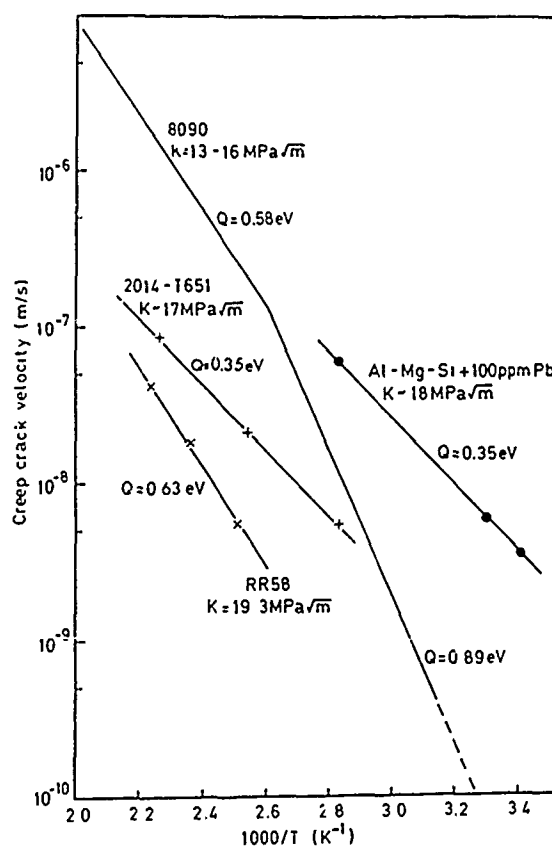

Fig 7 Arrhenius plots of S-L creep-crack-velocity versus inverse absolute temperature for 8090 and other aluminium alloys

Fig 8 Optical micrograph of section through specimen from the 25mm plate after creep crack growth at 120°C showing multiple, parallel, intergranular cracks
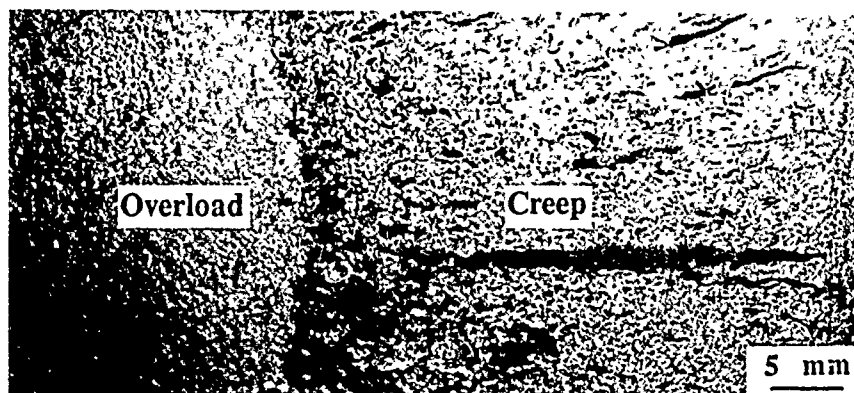
Fig 9 Macroscopic view of fracture surface produced by creep cracking at 120°C showing 'flaky' appearance
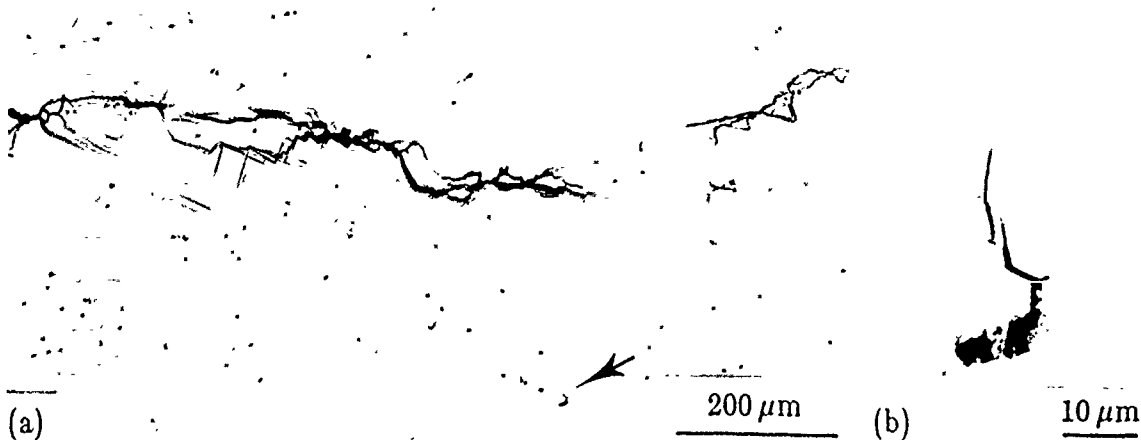
Fig 10 Optical micrographs of side surface of specimen from the experimental alloy with 40 ppm sodium after creep cracking at 80°C showing intergranular cracks initiated ahead of the main crack; inset shows cracking initiated from an inclusion in region arrowed
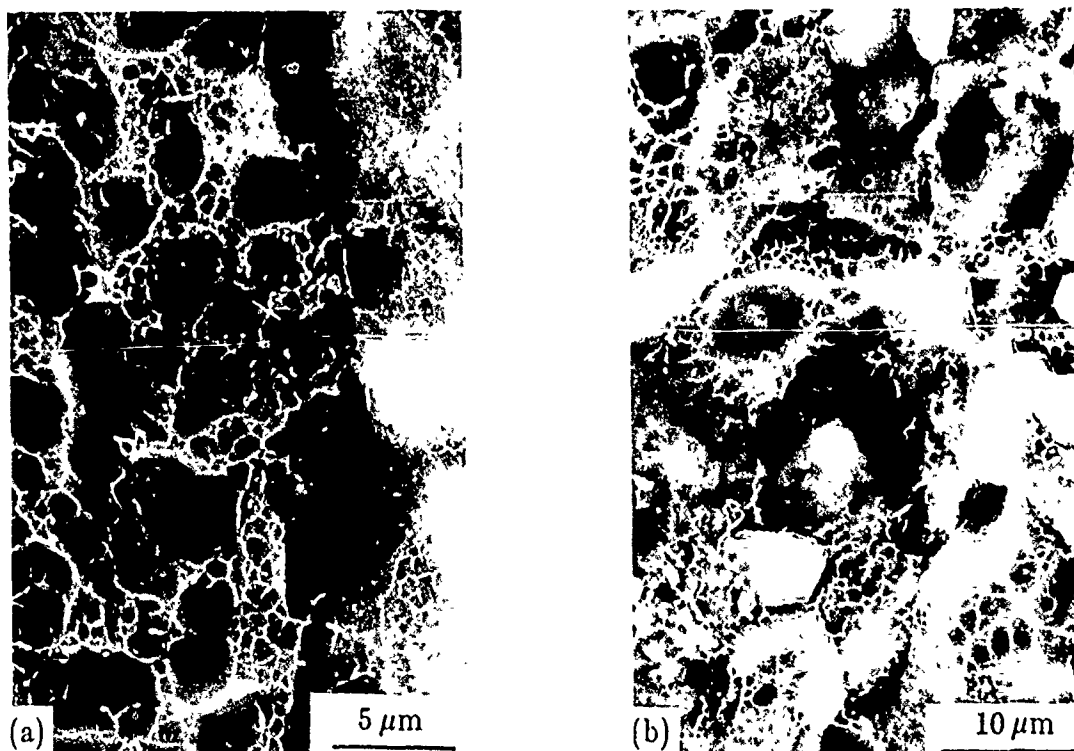
TR 90033

(a)   5 μm

(b)   10 μm

Fig 11   SEM of fracture surface of   (a) 25mm 8090 plate and   (b) experimental alloy
with 5-10 ppm sodium, showing brittle intergranular islands surrounded by
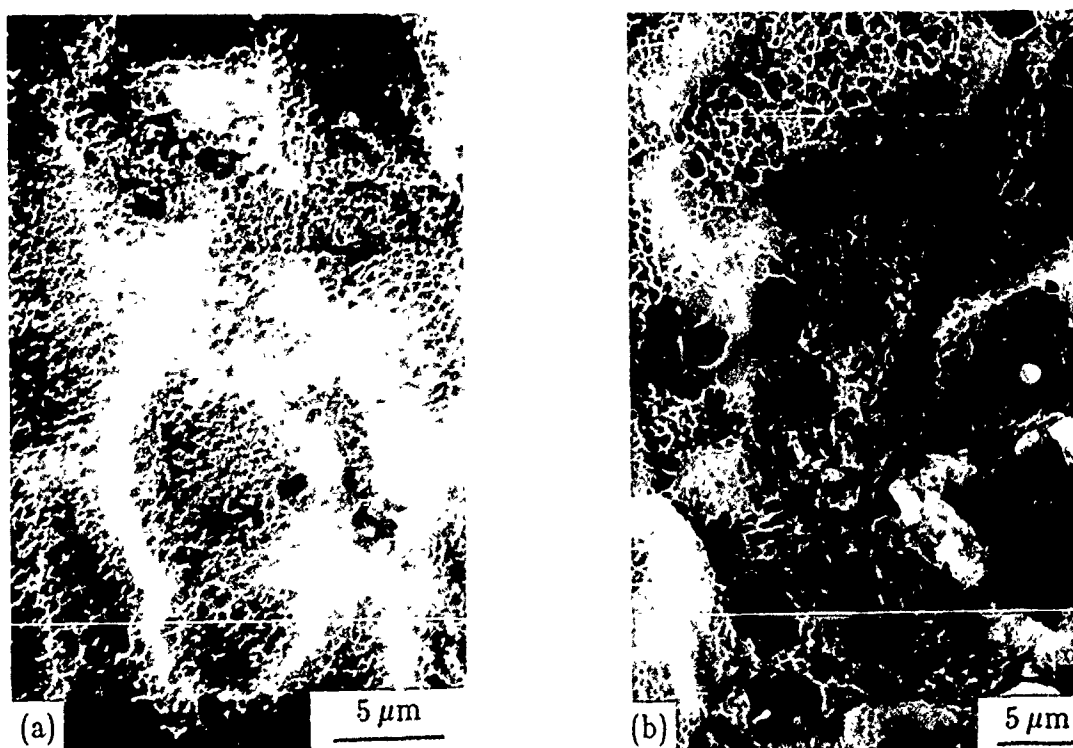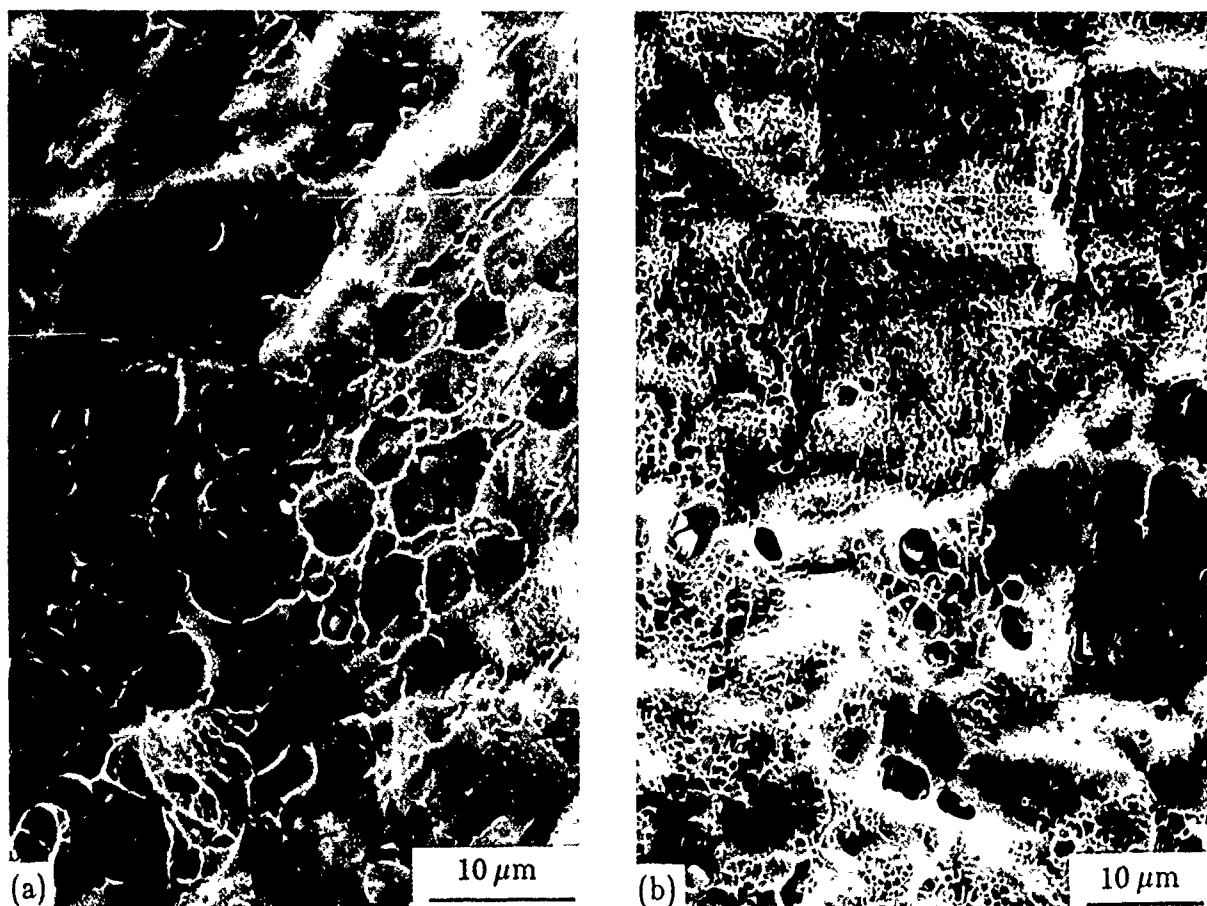dimpled regions produced by creep cracking at 120°C and at high K

(a)   5 μm

(b)   5 μm

Fig 12   SEM of fracture surface of   (a) 25mm 8090 plate showing dimpled inter-
granular areas produced by overload at 120°C, and   (b) experimental alloy
with ~10 ppm sodium showing brittle islands and dimpled areas produced
by overload at 20°C

TR 90033

Fig 13   SEM of fracture surface of experimental alloys with ~40 ppm sodium showing
(a) brittle intergranular islands produced by overload at 20°C, and
(b) predominantly dimpled areas produced by overload at -78°C
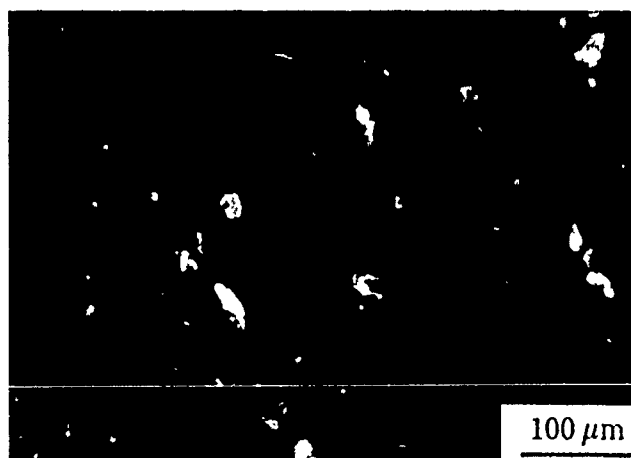
Fig 14   SIMS map using sodium ions of fracture surface of 25mm plate showing
(bright) sodium-rich areas. Surface diffusion of sodium has probably occurred
after fracture prior to analysis so that the areas are much larger than the
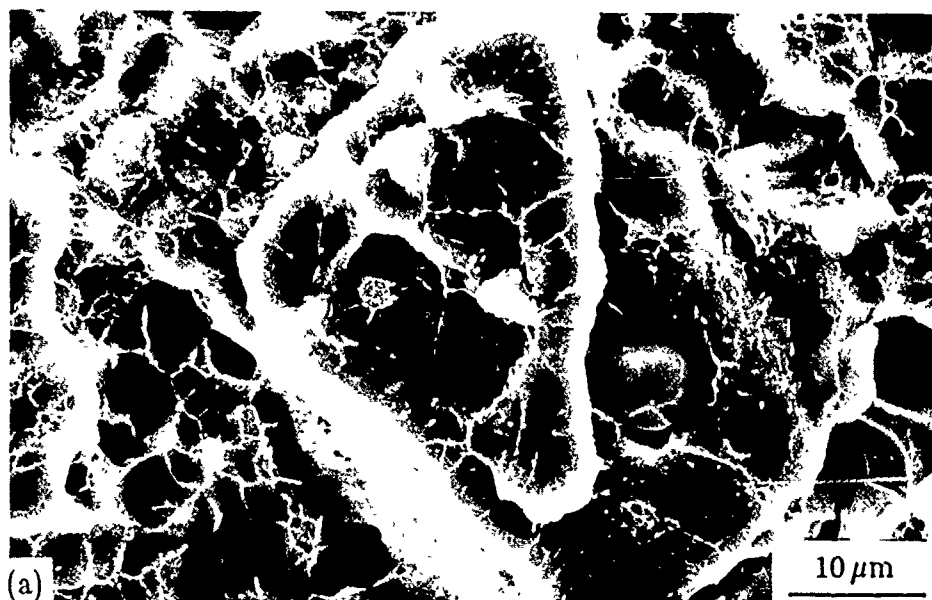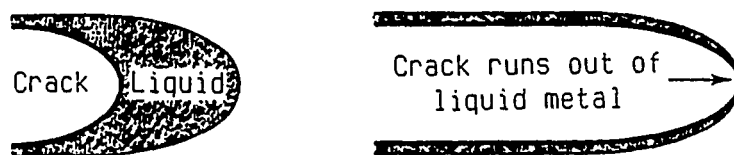original phases

TR 90033
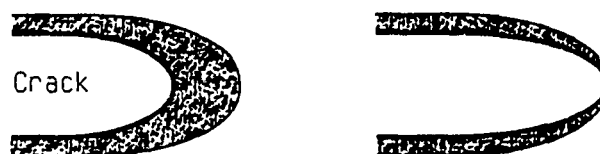
Fig 15 SEM of fracture surface of 2014-T651 plate showing dimples produced
(a) by creep cracking of 80°C, and (b) by overload at 20°C
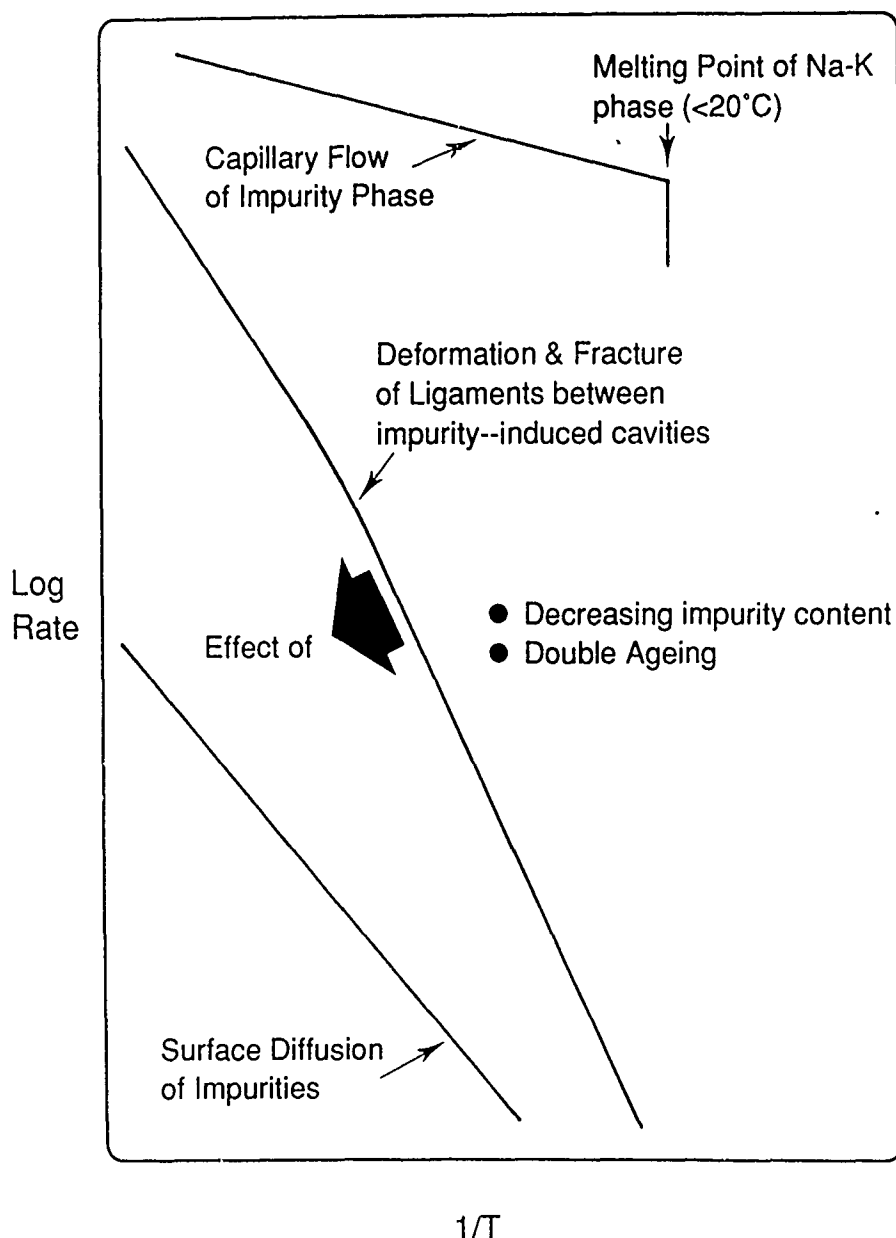
Fig 16

(a) Slow crack growth

(b) Rapid crack growth

Fig 16   Schematic diagrams illustrating the behaviour of liquid metal (shaded) at crack
tips during crack growth at   (a) low velocities and   (b) high velocities, for the
same small volume of liquid

Fig 17

The figure shows a schematic Arrhenius plot with axes labelled "Log Rate" (vertical) and "1/T" (horizontal). Labelled elements within the plot include: "Melting Point of Na-K phase (<20°C)", "Capillary Flow of Impurity Phase", "Deformation & Fracture of Ligaments between impurity--induced cavities", "Effect of", "• Decreasing impurity content • Double Ageing", and "Surface Diffusion of Impurities".

Fig 17   Schematic Arrhenius plots for the various processes involved in creep crack growth, as suggested by the present results. For consecutive processes, the slowest one is rate-controlling -- this is probably surface-diffusion of impurities to tips of cavities when impurity phases are solid (as in 2014), and probably deformation and fracture of ligaments between impurity-induced cavities when impurity phases are liquid (as in 8090). For the latter, rates decrease with: (i) decreasing impurity content, because the area of ligaments increases thereby decreasing the stress on ligaments, and (ii) double-ageing, which (temporarily) decreases lithium segregation at grain boundaries thereby increasing the creep-fracture resistance of ligaments

REPORT DOCUMENTATION PAGE

Overall security classification of this page

As far as possible this page should contain only unclassified information. If it is necessary to enter classified information, the box above must be marked to indicate the classification, e.g. Restricted, Confidential or Secret.

1. DRIC Reference (to be added by DRIC)	2. Originator's Reference RAE TR 90033	3. Agency Reference	4. Report Security Classification/Marking UNLIMITED
5. DRIC Code for Originator 7673000W	6. Originator (Corporate Author) Name and Location Royal Aerospace Establishment, Farnborough, Hants, UK		
5a. Sponsoring Agency's Code	6a. Sponsoring Agency (Contract Authority) Name and Location		

7. Title Sustained-load crack growth of 8090 aluminium-lithium alloy plate in dry air at 50-200°C

7a. (For Translations) Title in Foreign Language

7b. (For Conference Papers) Title, Place and Date of Conference

8. Author 1. Surname, Initials Lynch S.P.	9a. Author 2	9b. Authors 3, 4	10. Date July 1990	Pages	Refs. 26
11 Contract Number	12. Period	13. Project	14. Other Reference Nos. Mat/Str 288		

15. Distribution statement
    (a) Controlled by —

    (b) Special limitations (if any) —

If it is intended that a copy of this document shall be released overseas refer to RAE Leaflet No.3 to Supplement 6 of MOD Manual 4.

16. Descriptors (Keywords)   (Descriptors marked * are selected from TEST)

17. Abstract

    The effects of test temperature, stress-intensity factor, sodium impurity content, and ageing condition on the short-transverse sustained-load (creep) cracking of pre-cracked Al-Li-Cu-Mg-Zr (8090) alloy plate have been studied. Creep cracking was orders of magnitude faster, and threshold stress-intensity factors were much lower, than for conventional aluminium alloys such as 2014-T651. Significant rates of cracking were observed in 8090 alloys at temperatures as low as 60°C at stress-intensity factors as low as ~5 MPa$\sqrt{m}$. For a given stress-intensity factor, cracking rates were similar for underaged, peak-aged, and overaged conditions, but were higher for alloys with higher sodium impurity levels. Metallographic and fractographic observations suggest that the presence of liquid, sodium-rich impurity phases promote creep cracking in 8090 alloys. Creep cracking in conventional Al-alloys is probably exacerbated by solid impurity phases such as lead, which are less mobile and therefore less damaging than sodium-rich phases.

RAE Form A143 (revised October 1980)